

The Dynamics of Self-Trapped Beams of Incoherent White Light in a Free-Radical Photopolymerizable Medium

Jihua Zhang and Kalaichelvi Saravanamuttu*

Contribution from the Department of Chemistry, McMaster University, 1280 Main Street West, Hamilton, Ontario L8S 4M1, Canada

Received June 26, 2006; E-mail: kalai@mcmaster.ca

Abstract: Detailed experimental studies of the dynamics of self-trapped beams of white light (400–800 nm) in a photosensitive organosiloxane medium are presented. Self-trapped white light beams with similar spatial profiles formed in the organosiloxane at intensities ranging across an order of magnitude (2.7–22.0 W·cm⁻²). Beam-profiling measurements showed that these spatially and temporally incoherent wave packets propagate without diffracting (broadening) by initiating free-radical polymerization of methacrylate groups and corresponding refractive index changes in the organosiloxane medium. Analyses of their temporal evolution showed that the intensity-dependent behavior of self-trapped white light is similar to that of self-trapped laser light despite the extreme differences in their phase structure and chromaticity; the self-trapped incoherent beams even show the complementary oscillations of width and intensity that is characteristic of self-trapped coherent light. Furthermore, the dynamics of the self-trapped white light beams was found to be strongly correlated to the kinetics of free-radical polymerization and corresponding rates of refractive index changes in the organosiloxane. These studies provide accessible *photochemical* routes to self-trapped incoherent wave packets, which are extremely difficult to generate in conventional nonlinear optical media that owe their responses to higher-order dielectric susceptibility tensors. This could enable the experimental verification of theoretical models developed for the nonlinear propagation of white light and stimulate research into more complex self-trapping phenomena such as the interactions of self-trapped incoherent beams and spontaneous pattern formation due to modulation instability in a uniform incoherent optical field. These findings also carry potential for the development of self-induced waveguide, optical solder and interconnect technology for incoherent light emitted by incandescent sources or LEDs.

Introduction

Solitary waves that propagate over long distances without dissipating exist in diverse systems ranging from water waves, liquid crystals, plasmas, atmospheric clouds to crystalline lattices.¹ The optical equivalent—the self-trapped light beam—forms in media with nonlinear intensity-dependent changes in refractive index. Here, a beam induces a narrow waveguide through which it propagates without diffracting (broadening). While self-trapped coherent laser beams have been studied over four decades^{2–10} a recent topic is the self-trapping of *incoherent* light. Self-trapped light beams that are spatially—but *not*

temporally—incoherent have been extensively studied;^{11–20} their interactions^{21,22} and the formation of dark self-trapped beams^{23,24} have also been examined. Studies of *partially* incoherent wave packets have led to the fascinating problem of self-trapped light

- (1) Remoissenet, M. *Waves Called Solitons: Concepts and Experiments*; Springer-Verlag: Berlin, New York, 1994.
- (2) Segev, M.; Stegeman, G. I. *Phys. Today* **1998**, *51*, 42–48.
- (3) Stegeman, G. I.; Segev, M. *Science* **1999**, *286*, 1518–1523.
- (4) Bathelemy, A.; Maneuf, S.; Froehly, C. *Opt. Commun.* **1985**, *55*, 201–206.
- (5) Maneuf, S.; Desailly, R.; Froehly, C. *Opt. Commun.* **1988**, *65*, 193–198.
- (6) Aitchison, J. S.; Weiner, A. M.; Silberberg, Y.; Oliver, M. K.; Jackel, J. L.; Leaird, D. E.; Vogel, E. M.; Smith, P. W. E. *Opt. Lett.* **1990**, *15*, 471–473.
- (7) Trillo, S.; Torruellas, W., Eds. *Spatial Solitons*; Springer, New York, 2001; pp 87–125.
- (8) Aitchison, J. S.; Al-Hemiyari, K.; Ironside, C. N.; Grant, R. S.; Sibbet, W. *Electron. Lett.* **1992**, *28*, 1879–1880.
- (9) Bartuch, U.; Peschel, U.; Gabler, Th.; Waldhaus, R.; Horhold, H.-H. *Opt. Commun.* **1997**, *134*, 49–54.
- (10) Bjorkholm, J. E.; Ashkin, A. *Phys. Rev. Lett.* **1974**, *32*, 129–132.

- (11) Krolikowski, W.; Bang, O.; Wyller, J. *Phys. Rev. E: Stat., Nonlinear Soft Matter Phys.* **2004**, *70*(3 Pt 2), 036617/1–036617/5.
- (12) Shen, M.; Wang, Q.; Shi, J.; Hou, P.; Kong, Q. *Phys. Rev. E: Stat., Nonlinear Soft Matter Phys.* **2006**, *73*(5 Pt 2), 056602–056607.
- (13) Christodoulides, D. N.; Coskun, T. H.; Joseph, R. I. *Opt. Lett.* **1997**, *22*, 1080–1082.
- (14) Christodoulides, D. N.; Coskun, T. H.; Mitchell, M.; Segev, M. *Phys. Rev. Lett.* **1998**, *80*(11), 2310–2313.
- (15) Coskun, T. H.; Christodoulides, D. N.; Mitchell, M.; Chen, Z.; Segev, M. *Opt. Lett.* **1998**, *23*(6), 418–420.
- (16) Buljan, H.; Schwartz, T.; Segev, M.; Soljacic, M.; Christodoulides, D. N. *J. Opt. Soc. Am. B* **2004**, *21*(2), 397–404.
- (17) Makris, K. G.; Sarkissian, H.; Christodoulides, D. N.; Assanto, G. *J. Opt. Soc. Am. B* **2005**, *22*(7), 1371–1377.
- (18) Cohen, O.; Buljan, H.; Schwartz, T.; Fleischer, J. W.; Segev, M. *Phys. Rev. E: Stat., Nonlinear Soft Matter Phys.* **2006**, *73*(1–2), 015601/1–015601/4.
- (19) Mitchell, M.; Segev, M.; Coskun, T. H.; Christodoulides, D. N. *Phys. Rev. Lett.* **1997**, *79*, 4990–4993.
- (20) Katz, O.; Carmon, T.; Schwartz, T.; Segev, M.; Christodoulides, D. N. *Opt. Lett.* **2004**, *29*(11), 1248–50.
- (21) Petrović, M.; Jović, D.; Belić, M.; Schröder, J.; Jander, Ph.; Denz, C. *Phys. Rev. Lett.* **2005**, *95*(5), 053901-1–053901-4.
- (22) Stepken, A.; Kaiser, F.; Belić, M. R.; Krolikowski, W. *Phys. Rev. E: Stat., Nonlinear Soft Matter Phys.* **1998**, *58*(4), R4112–R4115.
- (23) Chen, Z.; Mitchell, M.; Segev, M.; Coskun, T. H.; Christodoulides, D. N. *Science* **1998**, *280*(5365), 889–892.
- (24) Christodoulides, D. N.; Coskun, T. H.; Mitchell, M.; Chen, Z.; Segev, M. *Phys. Rev. Lett.* **1998**, *80*, 5113–5116.

that is *both* spatially and temporally incoherent, such as white light emitted by the sun or tungsten filaments.⁷

Because it originates from the uncorrelated decay of excited states, white light suffers random phase and amplitude fluctuations on the femtosecond time scale.²⁵ Most detectors (including the human naked eye) due to their relatively long response times see only the time-averaged envelope of the incoherent beam. A focused white light beam *appears* to have a smooth, radially symmetric intensity profile but is actually composed of a distribution of bright and dark speckles that fluctuate randomly in space at the femtosecond time scale.²⁶ The counterintuitive phenomenon of an incoherent wave packet with extremely weak correlations of phase and amplitude traveling as a single, self-trapped entity has stimulated entirely new theoretical frameworks for nonlinear light propagation. These models have probed properties such as the spatial correlation distance, shape,²⁷ and frequency distribution²⁸ of self-trapped white light beams, described them in terms of geometric optics,²⁹ traced their evolution in media with nonlocalized responses³⁰ and their response to intensity fluctuations,³¹ predicted their existence in periodic nonlinear lattices³² as well as the spontaneous formation of patterns due to modulation instability of white light fields.³³

To physically *generate* self-trapped white light beams, three prerequisites were identified by theoretical models.^{7,28} The primary condition is a noninstantaneous photoresponse that is delayed with respect to the time of irradiation; index changes are therefore induced by the time-averaged intensity, in which random phase fluctuations are effectively canceled out. The second condition dictates that optical power be conserved; this means that the waveguide induced during self-trapping must be multimoded in order to support the multiple optical modes constituting white light. This requirement is refined in the third condition of self-consistency, which ensures that the beam is always confined to the self-induced waveguide. For this to be achieved, the total intensity resulting from the time-averaged distribution of waveguide modes must correspond to the time-averaged intensity of the white light beam. Because white light is itself composed of multiple modes, the time-averaged distribution of waveguide modes must also be correlated to the time-averaged distribution of modes of white light.

Refractive index changes due to typical nonlinear responses (e.g., Kerr³⁴ and Pockel's³⁵ effects) originate from electronic processes based on high-order dielectric susceptibility tensors. Resulting photoresponse times are therefore on the order of femtoseconds, which render them sensitive to phase fluctuations and disrupt self-trapping. The generation of self-trapped white

light beams in conventional nonlinear media is therefore a challenge. The first observation of self-trapped white light was made by Mitchell and Segev in a photorefractive crystal;²⁶ here, extremely low (nW) powers were employed in order to force a slow photoresponse from this nonlinear optical medium. Modulation instability—a phenomenon related to self-trapping—in a uniform field of white light was also observed under similar conditions.⁴⁶ With the exception of these seminal reports, experimental studies of the nonlinear propagation of light—that is *both* spatially and temporally incoherent—have until now been scarce. This is probably due to difficulties in generating self-trapped white light beams in conventional nonlinear media.

We recently demonstrated that the problem of ultrafast responses inherent to conventional nonlinear media is entirely avoided through a photochemical approach: self-trapped white light beams form due to index changes caused by photopolymerization of methacrylate groups in an organosiloxane gel.³⁶ This implies that the three prerequisites for self-trapping of white light are satisfied by the rate and magnitude of index changes in the organosiloxane.^{7,28} The most critical prerequisite of a noninstantaneous photoresponse is in fact an intrinsic property of the system. Because index changes originate from a diffusion-limited chemical reaction, the photoresponse time necessarily exceeds the femtosecond time scale. The organosiloxane therefore responds only to the time-averaged intensity—just as it would in the case of coherent light—which allows self-trapping of the rapidly fluctuating, multimode, polychromatic wave packet. The ability in this way to generate self-trapped white light beams has enabled the detailed investigation of their fundamental properties presented in this article. These studies examine the dynamics of self-trapped white light beams through careful control of the polymerization rates and resulting rates of refractive index changes in the organosiloxane.

Results and Discussion

Self-Trapping of Spatially and Temporally Incoherent White Light at Different Intensities. Self-trapping of white light in an organosiloxane medium was studied at seven different initial intensities (measured at the focal point) of the beam that ranged across an order of magnitude (2.7, 3.5, 5.4, 7.9, 12.1, 16.8, 22.0 W·cm⁻²). In a typical experiment, collimated white light (400–800 nm) from a QTH lamp was focused onto the entrance face of the medium. At this focal point (defined as 0.00 mm along the propagation axis *z*), the beam at all intensities had full width at half-maximum (fwhm) values of 49 and 45 μm in the transverse *x* and *y* directions, respectively; the evolution of its spatial profile at *z* = 6.00 mm was then monitored. Results of the highest (22.0 W·cm⁻²), two mid (7.9 and 5.4 W·cm⁻²), and lowest (2.7 W·cm⁻²) intensities are presented in Figure 1; corresponding parameters for all seven intensities are listed in Table 1.

The diffracted beam is broad, diffuse, and weak at all intensities (Figure 1a–d, Table 1). For example, the beam at 22.0 W·cm⁻² broadens from a fwhm (*y*) of 45 μm at *z* = 0.00 mm to 238 μm at *z* = 6.00 mm (Figure 1a). Large diffraction values are characteristic of white light, being a consequence of its random phase fluctuations—or incoherence. By contrast, a coherent, visible, continuous wave laser beam (400 nm) would

(25) Siegman, A. E. *Lasers*; University Science Books: Mill Valley, CA, 1996; p 50.

(26) Mitchell, M.; Segev, M. *Nature* (London) **1997**, *387*, 880–883.

(27) Buljan, H.; Šiber, A.; Soljačić, M.; Schwartz, T.; Segev, M.; Christodoulides, D. N. *Phys. Rev. E: Stat., Nonlinear Soft Matter Phys.* **2003**, *68*(3 Pt 2), 036607–036612.

(28) Buljan, H.; Segev, M.; Soljačić, M.; Efremidis, N. K.; Christodoulides, D. N. *Opt. Lett.* **2003**, *28*(14), 1239–1241.

(29) Snyder, A. W.; Mitchell, D. J. *Phys. Rev. Lett.* **1998**, *80*(7), 1422–1424.

(30) Shen, M.; Wang, Q.; Shi, J.; Chen, Y.; Wang, X. *Phys. Rev. E: Stat., Nonlinear Soft Matter Phys.* **2005**, *72*(2 Pt 2), 026604–026613.

(31) Ponomarenko S. A.; Litchinitser N. M.; Agrawal, G. P. *Phys. Rev. E: Stat., Nonlinear Soft Matter Phys.* **2004**, *70*(1 Pt 2), 015603–015606.

(32) Pezer, R.; Buljan, H.; Bartal, G.; Segev, M.; Fleischer, J. W. *Phys. Rev. E: Stat., Nonlinear Soft Matter Phys.* **2006**, *73*(5–2), 056608–056616.

(33) Buljan, H.; Šiber, A.; Soljačić, M.; Segev, M. *Phys. Rev. E: Stat., Nonlinear Soft Matter Phys.* **2002**, *66*(3), 035601–035604.

(34) Yeh, P. *Introduction to Photorefractive Nonlinear Optics*; Wiley: New York, 1993.

(35) Solymar, L.; Webb, D. J.; Grunnet-Jepsen, A. *The Physics and Applications of Photorefractive Materials*; Oxford: New York, 1996.

(36) Zhang, J.; Kasala, K.; Rewari, A.; Saravanamuttu, K. *J. Am. Chem. Soc.* **2006**, *128*, 406–407.

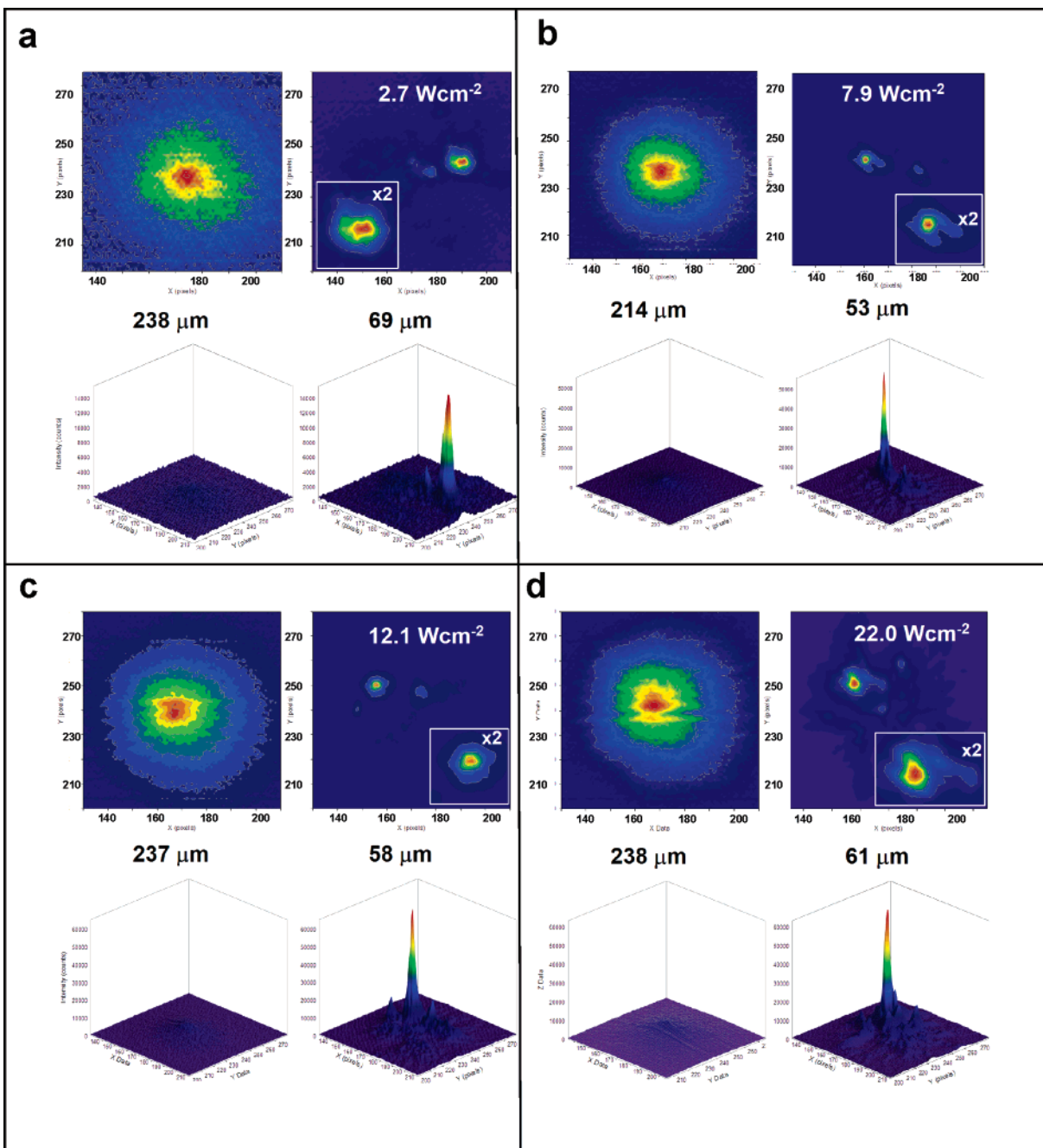


Figure 1. Two- (2-D) and three-dimensional (3-D) intensity profiles of diffracted and self-trapped beams of white light at (a) $2.7 \text{ W}\cdot\text{cm}^{-2}$, (b) $7.9 \text{ W}\cdot\text{cm}^{-2}$, (c) $12.1 \text{ W}\cdot\text{cm}^{-2}$, (d) $22.0 \text{ W}\cdot\text{cm}^{-2}$ with corresponding values of beam width (fwhm, y direction). The area containing all beam profiles were kept the same for ease of comparison. The inset is a 2-fold magnification of the 2-D profile of the self-trapped beam. The intensity scale was normalized to the maxima of all 2-D profiles of the diffracted beam to enhance visibility; the intensity scale of all other profiles in a given set was kept constant.

suffer near-field diffraction and broaden to only $137 \mu\text{m}$ under identical conditions. In the nonphotosensitized organosiloxane—in the absence of polymerization and thus under *linear* optical conditions—the white light beam remained diffracted for as long as it was monitored (up to 3000 s). However, in the medium that was photosensitized with titanocene free-radical photoinitiator ($\lambda_{\text{max}} = 393, 460 \text{ nm}$), the broad beam narrowed significantly in both transverse directions into an intense, focused peak. The beam remained thus self-trapped without reverting to its diffracted form for as long as it was monitored (1400 s).

Self-trapping was observed at all seven intensities. There is sharp contrast between the diffracted and narrowed beam profiles; the beam at $22.0 \text{ W}\cdot\text{cm}^{-2}$ for example narrowed from

a width of 249 to $65 \mu\text{m}$ (x direction) and from 238 to $61 \mu\text{m}$ (y direction) with at least a 7.3-fold increase in relative peak intensity (Figure 1a). The same 4-fold decrease in beam width (averaged for x and y directions) was observed during self-trapping at all intensities (Table 1). As a result, the spatial profiles of self-trapped beams—at intensities varying over an order of magnitude—are strikingly similar (Figure 1a–d).

The beam self-traps by initiating free-radical polymerization of methacrylate groups along the propagation axis. Resulting index changes are positive and strongly localized in space. (Lithographic studies showed that the spatial resolution of the photoresponse is $\sim 150 \text{ nm}$.³⁷) The beam, which has a fwhm of $45.0 \mu\text{m}$ at $z = 0.00 \text{ mm}$ at all studied intensities, induces a

Table 1. Widths^a (fwhm, in the *x* and *y* Transverse Directions) of the Diffracted and Self-Trapped Forms of White Light with Different Initial Intensities at a Propagation Distance of 6.00 mm in the Organosiloxane Gel

intensity [W·cm ⁻²] ± 0.1 W·cm ⁻²	diffracted fwhm [μm]		self-trapped fwhm [μm]		decrease in width [fold]
	<i>x</i>	<i>y</i>	<i>x</i>	<i>y</i>	
2.7	282	238	67	69	4
5.4	252	218	64	65	4
7.9	257	214	53	53	4
12.1	258	237	57	58	4
16.8	222	197	61	56	4
22.0	249	238	65	61	4

^a The ratio of the diffracted width to the self-trapped width of the beam is also listed.

narrow circular waveguide along *z*, populates the self-induced waveguide as guided optical modes, and propagates without broadening. Because the waveguide suppresses the natural diffraction of white light, the spatial profile of the beam no longer varies significantly from *z* = 0.00 to 6.00 mm. For all studied intensities, the self-trapped beam widths all fall in the narrow range between 53 to 69 μm (Table 1); in other words, their spatial profiles remain comparable to those at their original focal points (fwhm of 45 μm)—even after 6.00 mm of propagation.

The formation of self-trapped white light beams with similar spatial profiles *across a wide range of intensities* is especially significant considering the spatial and temporal incoherence of the optical field, which as detailed in the Introduction imposes nontrivial requirements on the photoresponse.^{7,28} As shown below, the remarkable tolerance of the organosiloxane to self-trapping of white light at different intensities is the direct consequence of methacrylate polymerization kinetics, and corresponding rates of refractive index changes.

Temporal Evolution of Self-Trapped Beams at Different Optical Intensities. To correlate self-trapping dynamics to polymerization kinetics, the time-dependence of self-trapping at different intensities was studied.³⁸ Temporal plots of efficiency and beam width (fwhm, *y* direction) during self-trapping are presented in Figure 2. To quantitatively compare plots corresponding to different intensities, the relative peak intensity of the beam was converted to an efficiency term, which is defined as the ratio of the relative peak intensity at a given time (*t*) to its value at *t* = 0 s. Changes in efficiency and beam width vary inversely in all temporal plots, indicating that optical power is conserved during the process.

Although the *spatial* profiles of self-trapped beams are similar at all intensities (Figure 1a–d, Table 1), plots in Figure 2 show that their *temporal* evolution is different. Each plot consists of three stages; the rates of change of efficiency and beam width within each stage however vary with intensity. For example, as shown in Figure 2a, the beam at 22.0 W·cm⁻² (i) increased in efficiency to >7.3 with a simultaneous decrease in width from 238 to 51 μm in only 74 s. Once self-trapped, the beam (ii) suffered oscillations of efficiency and width for 266 s before

(iii) decreasing to an efficiency of 2.9 in the next 1060 s. At experiment's end (1400 s), the beam remained self-trapped with an efficiency of 2.9 and a width of 72 μm—this is a 3.3-fold decrease relative to its diffracted width at *t* = 0 s. The rates and magnitude of corresponding changes at 2.7 W·cm⁻² were different (Figure 2d): the beam (i) showed an increase in efficiency to 7.8 and decrease in width from 238 to 65 μm in the first 345 s, (ii) oscillated about this high efficiency for 232 s before (iii) decreasing in efficiency to 1.3 with a corresponding increase in width to 130 μm over the next 823 s. At 1400 s, the self-trapped beam had an efficiency of 1.27 and a width of 130 μm, which corresponds to a 1.8-fold decrease relative to its diffracted width.

The three stages (i–iii) of self-trapping are evident in the temporal plots of all studied intensities (Figure 2) and are a means to compare self-trapping at different intensities; parameters corresponding to each stage are listed in Table 2. Physically, stages (i–iii) represent the (i) self-focusing, (ii) self-trapping, and (iii) waveguide formation sequence that constitute the self-trapping process.³⁶ In stage (i), the beam induces a refractive index gradient—a lens—at *z* = 0.00 mm and focuses along the propagation axis. At *z* = 6.00 mm, where the beam would diffract under linear conditions, self-focusing causes rapid increase in efficiency and decrease in beam width. Values in Table 2 show that the duration of stage (i) is always short (74 to 345 s) relative to the time-scale (1400 s) of the entire self-trapping process. In stage (ii), self-lensing and self-focusing of the beam along *z* lead to the formation of a channel waveguide with a gradient index profile. The waveguide traps the beam with high efficiency and suppresses divergence; as observed in Table 2, the maximum efficiency of self-trapping (ranging from 6.7 to 11.9) always occurred in stage (ii). Refractive index changes saturate in stage (iii) as methacrylate groups are depleted by polymerization. The gradient in refractive index is therefore erased, and the waveguide develops a uniform (step-index) profile. Confinement of white light in the step-index relative to a gradient-index waveguide is weak; the consequent increase in the evanescent component of the self-trapped optical field causes polymerization in regions surrounding the waveguide.³⁹ The waveguide broadens, and optical power is distributed over a larger cross-section, as observed by the increase in width and decrease in efficiency of the beam in stage (iii). Plots in Figure 2 and efficiency values listed in Table 2 show that, despite the broadening of waveguides, beams at all intensities showed greater efficiency and smaller widths relative to their diffracted forms at *t* = 0 s and therefore remained self-trapped at experiment's end (1400 s).

Stages (i) and (iii) of the Self-Trapping Process. The temporal evolution of the self-trapped beam at different intensities is distinguished by two main features—the duration of stage (i) and the nature of its oscillations, which dominate stage (ii) and (for weaker beam intensities) stage (iii) of the process. Differences in stage (i) are considered first.

The most significant changes to beam width and efficiency take place in stage (i)—it is at the completion of stage (i) that the beam first self-traps. Self-trapped beams at all studied intensities possess similar spatial profiles (Figure 1) and, because the emission spectrum of the QTH source does not change

(37) Saravanamuttu, K.; Blanford, C. F.; Sharp, D. N.; Dedman, E. R.; Turberfield, A. J.; Denning, R. G. *Chem. Mater.* **2003**, *15*, 2301–2304.

(38) Real-time monitoring of the self-trapping process is possible only because the photoresponse time of the organosiloxane—determined by typical polymerization rates—is on the order of milliseconds to minutes. In a conventional nonlinear optical material such as a Kerr medium with a photoresponse on the order of femtoseconds, studies of the temporal evolution of self-trapping are impossible.

(39) Marcuse, D. *Theory of Dielectric Optical Waveguides*; Academic Press: New York, 1991.

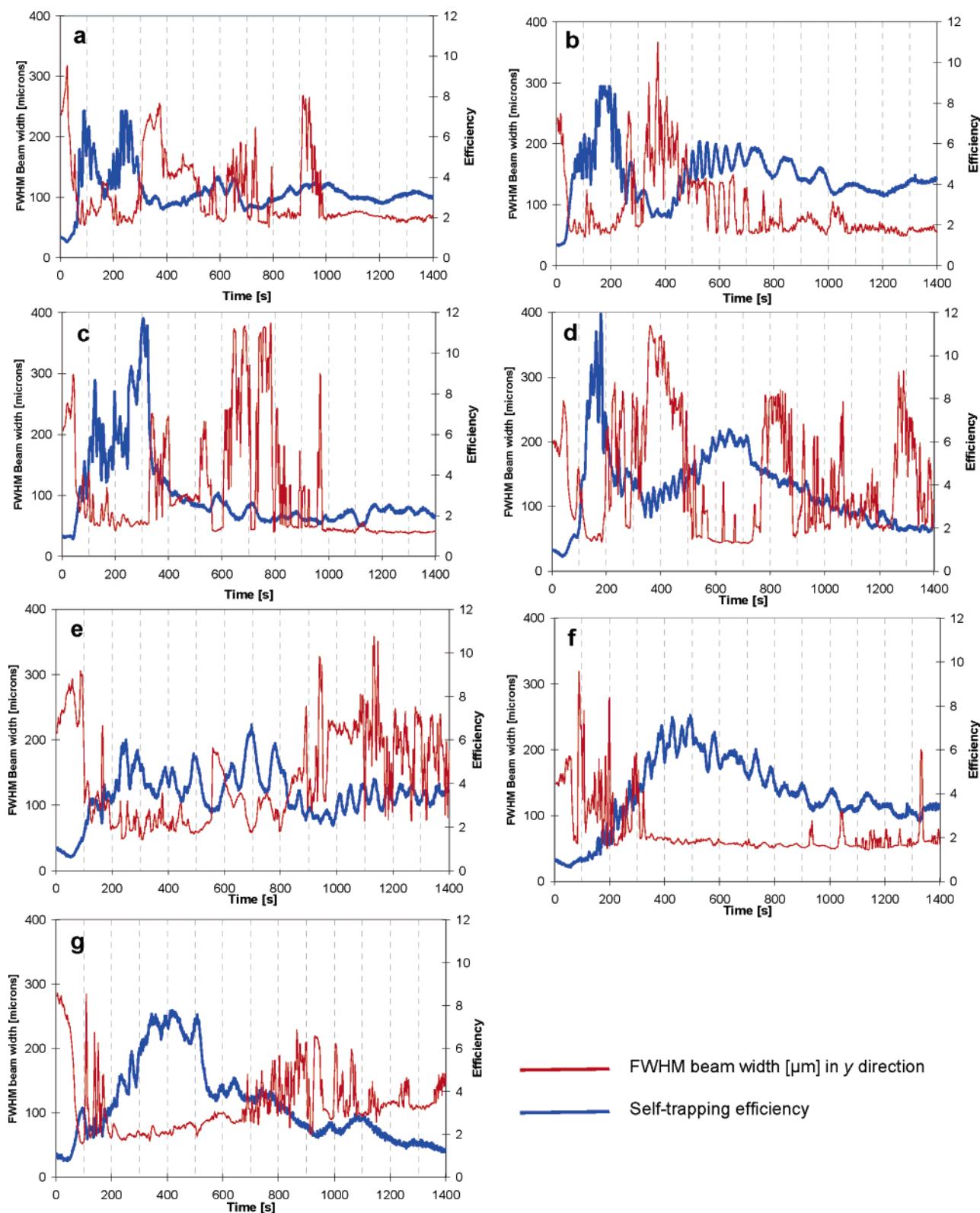


Figure 2. Temporal evolution of the efficiency and fwhm beam width (y direction) at a propagation distance of 6.00 mm during the self-trapping of white light at initial intensities of (a) 22.0 W·cm⁻², (b) 16.8 W·cm⁻², (c) 5.4 W·cm⁻², (d) 12.1 W·cm⁻², (e) 7.9 W·cm⁻², (f) 3.5 W·cm⁻², and (g) 2.7 W·cm⁻².

significantly over this intensity range, are composed of the same range of visible wavelengths (400–800 nm). Self-trapped beams with similar widths and spectral composition but different intensities can exist only if the profile and magnitude of the induced refractive index is the same.⁴⁰ This means that the

spatial profile (gradient) and *magnitude* of refractive index changes induced along z during stage (i) are the same at all intensities.

Because the polymerization rate is proportional to intensity, the refractive index gradient induced in stage (i) should

Table 2. Parameters Corresponding to the Temporal Evolution of White Light Self-trapping at Different Initial Intensities, Including the Duration of Stage (i), the Maximum Efficiency of Self-trapping and Corresponding Beam Widths (in the x and y Transverse Directions) and Time in Stage (ii), and the Final Efficiency at the End of the Experiment (1400 s)

intensity [W·cm ⁻²] ± 0.1 W·cm ⁻²	stage (i) [s]	maximum self-trapping efficiency	self-trapped width at maximum efficiency		time of maximum efficiency [s]	final efficiency (at 1400 s)
			x	y		
2.7	345	7.8	66	65	416	1.3
3.4	338	7.6	49	58	493	3.4
5.4	239	6.7	67	54	697	3.9
7.9	131	11.9	45	45	179	2.2
12.1	109	11.7	49	55	304	1.9
16.8	70	> 8.8	49	51	161	4.3
22.0	74	> 7.3	61	51	90	2.9

correspond to the spatial profile of the roughly Gaussian beam at $z = 0.00$ mm. However, such an index *gradient* is possible only if the photoresponse is strongly localized in space. This condition is satisfied by typical nonlinear processes such as the Kerr effect, in which index changes originate from higher-order susceptibility tensors and the photoresponse is strictly localized to the incident field; the spatial profile of the index change therefore exactly matches the beam profile. The photoresponse of the organosiloxane however is not electronic in nature but is due to a polymerization process; the index change at a specific point of the incident optical field is therefore necessarily delocalized over a characteristic volume ($4/3\pi r^3$) in which a polymer chain forms. In contrast to free monomer systems,⁴¹ diffusion of free-radical propagators is inhibited in the organosiloxane in which methacrylates are covalently bound to siloxane oligomers. As a result, the delocalization (r)—or spatial resolution—of the photoresponse is only ~ 150 nm.³⁷ To approximate the index profile induced in this medium, a Gaussian profile with a fwhm value of $45 \mu\text{m}$ was averaged—or *blurred*—over 150-nm intervals (Figure S3, Supporting Information). No significant difference was found between the two normalized profiles; physically, this means that the white light beam (regardless of intensity) can induce a *gradient in refractive index change*—or lens—corresponding to its spatial profile at 0.00 mm. Because the spatial profile (gradient in intensity) of the beam at $z = 0.00$ mm is approximately the same at all intensities, the corresponding *gradient* of the refractive index change must also be the same.

However, the *magnitude* of the refractive index change induced in a given period of time (t) and volume (defined by x , y , z) in the organosiloxane varies with optical intensity as described by the empirically derived equation:^{42a–b}

$$\Delta n(x,y,z,t) = \Delta n_0 \left\{ 1 - \exp \left[-\frac{1}{U_0} \int_0^{t-\tau} |E(t)|^2 dt \right] \right\} \quad (1)$$

where Δn represents the change in refractive index at a particular point in time (t) and over a specific volume (defined by x , y , z), Δn_0 is the refractive index change at saturation, τ is the acrylate

(40) This is understood by considering that in linear optics, regardless of intensity, the same degree of focusing (or confinement) of light from the same source can only be achieved with a lens (or waveguide) with the same refractive index profile.

(41) It is important to note that a significantly delocalized photoresponse of the medium would lead to broader, weaker waveguides that support wider and less intense beams. This would be the case with photopolymerization of free monomer molecules; the large diffusion coefficients of free-radical propagators would cause severe blurring or even complete erasure of the gradient in refractive index changes that is necessary for self-trapping.

(42) (a) Kewitsch, A.; Yariv, A. *Opt. Lett.* **1996**, *21*, 24–26. (b) Kewitsch, A., Yariv, A. *Appl. Phys. Lett.* **1996**, *68*, 455–457.

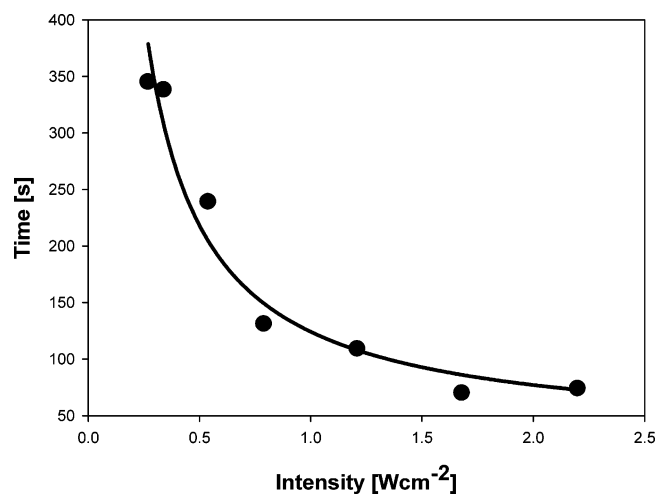


Figure 3. Plot of the duration of stage (i) of self-trapping against the initial intensity of the white light beam.

radical lifetime, U_0 is the critical optical exposure above which polymerization can be initiated and $|E(t)|^2$ is the square of the electric field amplitude, which is proportional to the intensity (I) of the optical field. Equation 1 shows that below the saturation limit (Δn_0) and at the typically negligible values of radical lifetimes the product of the incident optical intensity (I) and the time of exposure (t)—the total energy—to induce a specific refractive index change delocalized over a specific volume must be the same. The duration of stage (i)—that is, the time taken for the self-trapped beam to form—is the time of optical exposure necessary to induce *both* the gradient and magnitude of the index change (averaged across the gradient profile) required for self-trapping. Because this time is inversely proportional to intensity (eq 1), there is an inverse relationship between the duration of stage (i) and the intensity of the beam (Figure 3). This is an exact expression of the proportionality between the magnitude of refractive index change—or rate of polymerization—and optical intensity.

A correlation between polymerization kinetics and self-trapping dynamics can also be drawn in stage (iii). Efficiencies at experiment's end (1400 s) range between 1.3 and 4.3 with no noticeable trend with intensity (Table 2). This is because the refractive index change of self-induced waveguides evolves (at intensity-dependent rates) to the *same* uniform saturated value of approximately 0.006, characteristic of the organosiloxane medium.⁴³ At the end (or long times) of self-trapping, there is no significant difference between the spatial profiles of

(43) Saravanamuttu, K.; Du, X. M.; Najafi, S. I.; Andrews, M. P. *Can. J. Chem.* **1998**, *76*, 1717–1729.

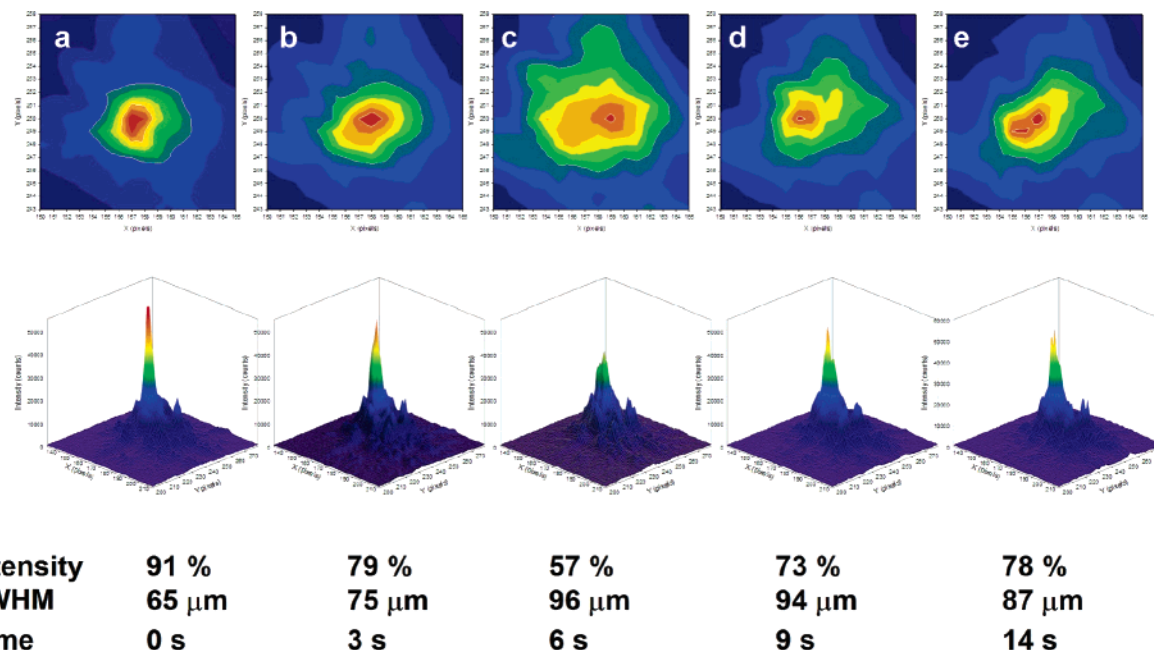


Figure 4. Changes to the spatial profile of the self-trapped beam at $22.0 \text{ W}\cdot\text{cm}^{-2}$ within the 14 s duration of a single oscillation. Each pixel has an area of $9.3 \mu\text{m} \times 9.3 \mu\text{m}$.

waveguides induced at different intensities and thus no significant difference—or at least a discernible trend with initial intensity—of self-trapping efficiency.

Stage ii: Oscillations of Efficiency and Width of the Self-Trapped Beam. Stages (i) and (iii) of self-trapping lead to *similar* overall changes in beam profiles, which are achieved at intensity-dependent rates. Stage (ii) is different; temporal plots in Figure 3 show that overall changes of beam profiles in this intermediate regime are not the same at all intensities. A first indication of this difference is found in values of maximum self-trapping efficiency listed in Table 2, which range from 6.7 to 11.9 (maximum efficiencies at the highest two intensities, 16.8 and $22.0 \text{ W}\cdot\text{cm}^{-2}$ could not be accurately determined due to detector saturation but are ≥ 8.8 and ≥ 7.3 , respectively). The largest change in maximum efficiency (5.2) occurred between self-trapping at 5.4 and $7.9 \text{ W}\cdot\text{cm}^{-2}$. Values of maximum efficiency between 7.9 and $12.1 \text{ W}\cdot\text{cm}^{-2}$ vary only by 0.2, whereas the variation in maximum efficiency for self-trapping between 5.4 and $2.2 \text{ W}\cdot\text{cm}^{-2}$ is 1.1. The abrupt and unusually large change in maximum efficiency between 5.4 and $7.9 \text{ W}\cdot\text{cm}^{-2}$ was observed in three separate series of intensity-dependent self-trapping experiments: the average change in maximum efficiency between 5.4 and $7.9 \text{ W}\cdot\text{cm}^{-2}$ was 7. The average change in maximum efficiencies at intensities between 7.9 and $22.0 \text{ W}\cdot\text{cm}^{-2}$ and separately, between 5.4 and $2.7 \text{ W}\cdot\text{cm}^{-2}$ were only 0.8 and 3.3, respectively.

Any variation at all of maximum efficiency with intensity is unexpected; the 4-fold decrease in beam width observed during self-trapping at all intensities (Figure 1, Table 1) implies that the maximum efficiencies—maximum change in beam intensity—should also be similar. A physical reason for this discrepancy is contained in the two-dimensional (2-D) intensity profiles of self-trapped beams at 7.9 and $5.4 \text{ W}\cdot\text{cm}^{-2}$ (Figure S4, Supporting Information). For the self-trapped beam at $5.4 \text{ W}\cdot\text{cm}^{-2}$, one-tenth of the intensity is distributed over a significantly larger area ($\sim 21360 \mu\text{m}^2$) compared to the beam at $7.9 \text{ W}\cdot\text{cm}^{-2}$ ($\sim 3200 \mu\text{m}^2$)—the waveguide induced at the smaller intensity

is less efficient because it traps a smaller proportion of light in its core. The inverse relationship between optical intensity and stage (i) means that the diffracted beam narrows more slowly at smaller intensities. During the self-trapping of weak beams, a larger area of the medium is therefore exposed to (relatively weak) light for longer times and as a result, may undergo index changes. The contrast in refractive index between the final self-induced waveguide and its surrounding medium is therefore weaker, leading to greater loss—leakage—of intensity from the waveguide.³⁹ This leads to a general decrease in self-trapping efficiency at smaller optical intensities.

Differences in the duration of stage (i) alone cannot account for the abrupt and large change in the maximum efficiency between 5.4 and $7.9 \text{ W}\cdot\text{cm}^{-2}$. This change appeared to be linked to oscillations of the self-trapped beam observed in all temporal plots in Figure 2. Oscillations typically begin at the completion of state (i) and persist, particularly in the case of smaller intensities, into stage (iii) of the process. Figure 4 contains 2-D and 3-D spatial profiles acquired during a *single* 14 s-long oscillation of the self-trapped beam at $22.0 \text{ W}\cdot\text{cm}^{-2}$. Because optical power is conserved during self-trapping, changes to relative peak intensity and width during the oscillation are complementary; the self-trapped beam appears to breathe as it expands from a width of $65 \mu\text{m}$ (with relative peak intensity of 91%) to a width of $96 \mu\text{m}$ (with a corresponding decrease in relative peak intensity to 57%) and narrows back to a width of $87 \mu\text{m}$ (relative peak intensity of 78%) in a period of 14 s. Table 3 lists parameters of oscillatory behavior derived from temporal plots in Figure 2; the average duration and amplitude of oscillations, and the length of time over which they were measured are listed. Although oscillations are periodic at early times, they gradually dampen (decrease in depth and increase in duration) with time. The average duration listed in Table 3 is therefore a relative measure (and not an indication of the periodicity) of oscillations. The average duration of oscillations for self-trapped beams with initial intensities of 22.0, 16.8, and $12.1 \text{ W}\cdot\text{cm}^{-2}$ is the same (17 s). The duration of oscillations at

Table 3. Average Duration and Average Amplitude of the Oscillations of Self-Trapped Beams and the Interval in Which They Were Measured for Different Optical Intensities

intensity [W·cm ⁻²] ± 0.1 W·cm ⁻²	interval measured [s]	average duration [s]	average amplitude
2.7	378 to 578	67	1.5 ± 0.5
3.4	352 to 820	52	1.3 ± 0.1
5.4	165 to 891	64	1.7 ± 0.2
7.9	93 to 342	27	1.8 ± 0.5
12.1	78 to 343	17	1.7 ± 0.5
16.8	64 to 355	17	1.4 ± 0.2
22.0	52 to 277	17	1.7 ± 0.5

the relative low intensities of 3.4 and 2.7 W·cm⁻² are 52 and 67 s, respectively. The largest change in average duration is 37 s, which occurs between intensities 7.9 and 5.4 W·cm⁻²; *this coincides with the point at which the largest change in the maximum efficiency of self-trapping was measured.*

The oscillatory behavior of both self-trapped incoherent³⁰ and coherent⁴⁴ beams have been theoretically predicted. The model of self-trapping developed by Snyder and co-workers⁴⁴ in particular provides insight into the intensity-dependent oscillatory behavior and particularly abrupt changes in maximum efficiency of self-trapped white light observed in our experiments. The model considers a slightly delocalized photoreponse, which allows the corresponding index change to be expressed as a function of intensity integrated over the photoreponse area—in other words, optical power. Power-dependent functions of refractive index provided simple solutions of the nonlinear Schrödinger equation, which describes—in the case of electromagnetic waves—light propagation under nonlinear conditions. The model cannot be applied to Kerr-type nonlinear media that exhibit strongly spatially localized and therefore intensity-dependent changes in refractive index, making self-trapped solutions difficult to obtain.

A slightly delocalized photoreponse is, however, characteristic of the organosiloxane; the observed behavior of self-trapped white light in this medium is in fact consistent with predictions of the Snyder model—even though the model considers a *coherent* Gaussian laser beam. For example, solutions of the model exhibit oscillations of intensity and width of self-trapped beams at a range of powers. Oscillations originate from the sequential refraction (focusing) and diffraction of the self-trapped beam along the propagation axis. The model showed that the refraction/diffraction *sequence* varies with power; refraction precedes diffraction at greater powers with the opposite taking place at smaller powers. A physical explanation for this sequence reversal is that index changes required for focusing are induced faster at greater powers. (The same reason underlies the inverse relationship between the duration of stage (i) and optical intensity of self-trapped white light beams (Figure 3).) The Snyder model further implies that the oscillation period increases at lower powers, which is consistent with the inverse trend between the average duration of oscillation and intensity observed for self-trapped white light (Table 3). Experimental data listed in Table 3 provide insight into the physical reason for this trend: the average oscillation amplitude is the same within error at different intensities—this means that the relative change in self-trapping efficiency between the trough (e.g., Figure 4c) and the peak (e.g., Figure 4a) of each oscillation is

approximately the same. The same change in efficiency is possible only if the index change induced during the oscillation is also the same. Longer times are required to induce a given index change at smaller intensities (eq1); the duration of oscillations is therefore greater at smaller intensities (Table 3).

Most significantly, the Snyder model locates a critical intermediate power—this is the point at which the refraction/diffraction sequence of the oscillating self-trapped beam is actually reversed. At this power, the refraction of the beam *exactly* cancels its own diffraction, and the self-trapped beam propagates without any changes to its spatial profile—this is the optical soliton. In the case of white light, the abrupt and large changes in the average duration of oscillations and maximum efficiency observed between 5.4 and 7.9 W·cm⁻² strongly suggest that self-trapped beams at these intensities exist on either side of such a critical intensity, (which when integrated over the spatial resolution of the organosiloxane photoreponse converts to critical power). Below this critical value, rates of index changes are small, and the beam diffracts before refractive index changes are sufficient for focusing—as observed by the longer durations of oscillations below 5.4 W·cm⁻². Above this value, rates of index changes are greater, and the opposite sequence takes place within a shorter period of time (>5.4 W·cm⁻²). The incandescent source employed in these experiments does not allow for resolution of intensities between 5.4 and 7.9 W·cm⁻². However, the above findings strongly indicate the existence of a critical intensity between these two values at which the self-trapped beam would propagate without any perturbation to its spatial profile—such a beam would be the spatially and temporally incoherent equivalent of the optical soliton.

Our findings show strong agreement between the *behavior* of self-trapped incoherent white light and that predicted for self-trapped coherent laser light—*despite* their fundamentally different optical structure and spectral composition. Similarities in the oscillatory behavior are particularly striking. In the case of laser light, oscillations correspond to periodic variations in intensity and width of a quasi-monochromatic light beam with strong spatial and temporal correlation of phase and amplitude. In the case of white light, oscillations are *collective* changes of a rapidly fluctuating, polychromatic wave packet with extremely weak correlations in phase and amplitude. The behavioral similarities of the coherent and incoherent self-trapped beams underscore the insensitivity of the organosiloxane to the incoherence of white light. To reiterate, the insensitivity is inherent to the mechanism underlying index changes in the medium, free-radical polymerization, which is governed by only the time-averaged intensity of the optical field (at the absorption wavelengths of the titanocene photoinitiator). We have shown that this in turn allows the dynamics—that is, the evolution of the self-trapped beam (stage (i)) and their temporal behavior once self-trapped (stages (ii to iii))—to be described and understood through the simple kinetics of free-radical polymerization (and the rates of corresponding refractive index changes).

Effect of Varying Concentrations of Methacrylate Groups.

To reinforce the correlation of polymerization kinetics to self-trapping dynamics, self-trapping was studied in organosiloxanes in which polymerization rates were now varied through the concentration of methacrylate groups. (At the same incident

(44) Snyder, A. W.; Mitchell, D. J. *Science* **1997**, *276*, 1538–1541.

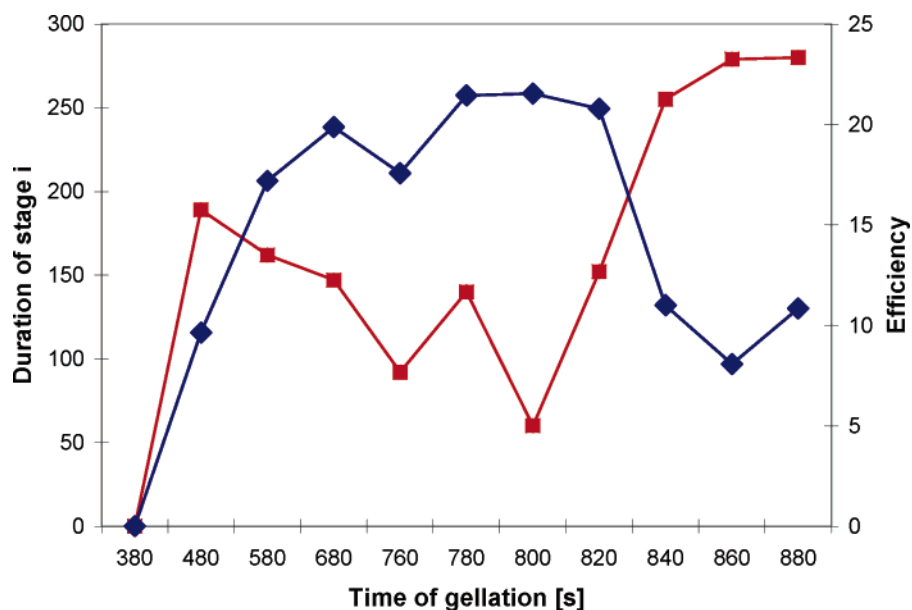


Figure 5. Plots of the duration of stage (i) (red) and maximum efficiency (blue) of self-trapping in gels formed by irradiation of organosiloxane sols for different lengths of time. (The corresponding table of values is provided as Supporting Information.)

optical intensity, rates of polymerization, and corresponding rates of refractive index changes are proportional to the concentration of polymerizable unit.)⁴⁵ Gels with different methacrylate concentrations were prepared by uniformly pre-irradiating the organosiloxane sol with white light (400–800 nm, 160 mW) to partially polymerize (and deplete) methacrylate groups prior to self-trapping experiments. Self-trapping of white light at 22.0 W·cm⁻² was studied in gels that had been pre-irradiated for times varying from 380 to 880 s. Our objective here was to qualitatively observe the trend of self-trapping in media with decreasing polymerization rates.

Self-trapped beams formed in all samples except in the one pre-irradiated for only 380 s. Temporal plots of self-trapping and a table of corresponding parameters are provided in Figure S5 of Supporting Information. Figure 5 contains plots of stage (i) and maximum efficiency of self-trapping versus time of pre-irradiation (decreasing methacrylate concentration). The duration of stage (i) varies inversely with maximum efficiency; the smallest duration of stage (i) (60 s) and largest value of maximum efficiency (21.5) occur in the sample irradiated for 800 s. In gels irradiated for times ≥ 800 s, there is an overall decrease in maximum efficiency (from 21.5 to 10.8) and a simultaneous increase in the duration of stage (i) (from 152 to 280 s). The self-trapping dynamics in this set of samples is also consistent with polymerization kinetics; the duration of stage (i) increases due to the decrease in polymerization rates (and consequent index changes) at smaller methacrylate concentrations (eq 1). There is an overall decrease in maximum efficiency because the maximum possible index change (Δn_0 in eq 1) is necessarily reduced at smaller methacrylate concentrations. This leads to a weaker contrast in refractive index between the self-induced waveguide and its surrounding medium. The confinement of intensity is consequently weaker and leads to a decrease in self-trapping efficiency.

Self-trapping dynamics follows the opposite trend in samples irradiated for times ≤ 800 s. Here, the duration of stage (i)

decreases and maximum efficiency increases with decreasing methacrylate concentration. This behavior suggests that, in addition to methacrylate concentration, self-trapping also depends on the viscosity of the medium. The extent of gelation and thus viscosity of the organosiloxane increases with time of irradiation as the medium gradually transforms from a fluid sol to a gel. In fact, below irradiation times of 500 s, the white light beam behaves as it would in a linear medium. This suggests that a viscosity threshold must be reached in order for self-trapping to occur.

Trapping White Light with a Uniform External Field. The dependence of self-trapping on both methacrylate concentration and viscosity of the medium provides a unique means to control beam propagation with an *external* optical field. Figure 6 contains spatial profiles (a–e) of a white light beam at 22.0 W·cm⁻² at a propagation distance of 6.00 mm in an organosiloxane sol that was being simultaneously irradiated with a (separate) uniform field of white light (400–800 nm, 160 mW). A table of the beam width and efficiency corresponding to each image (a–e) is also included. (The entire temporal plot of efficiency and width (fwhm, y) of the beam is presented as Figure S5 in Supporting Information; times corresponding to each spatial profile in Figure 6 (a–e) are indicated with dotted lines.) Unlike the typical self-trapping process, changes to the beam under uniform irradiation are rapid and appear to be reversible; the beam remains diffracted at early times when the organosiloxane is fluid. At 500 s, however, the medium begins to gel, and there is a sudden increase in efficiency, which maximizes at 23 at 794 s at a minimum beam width of 53 μm (Figure 6d). This is followed by a gradual decrease in efficiency and simultaneous increase in beam width; at 980 s, the beam reverts to a broad and weak form, with a width of 290 μm and an efficiency of only 3 (Figure 6e).

The temporal variation of efficiency during this process closely corresponds to the plot of maximum efficiency versus time of *pre*-irradiation (Figure 5)—each value of maximum efficiency in the latter was derived from *individual* self-trapping processes in gels prepared at different irradiation times. For

(45) Decker, C. *Polym. Int.* **1998**, *45*, 133–141.

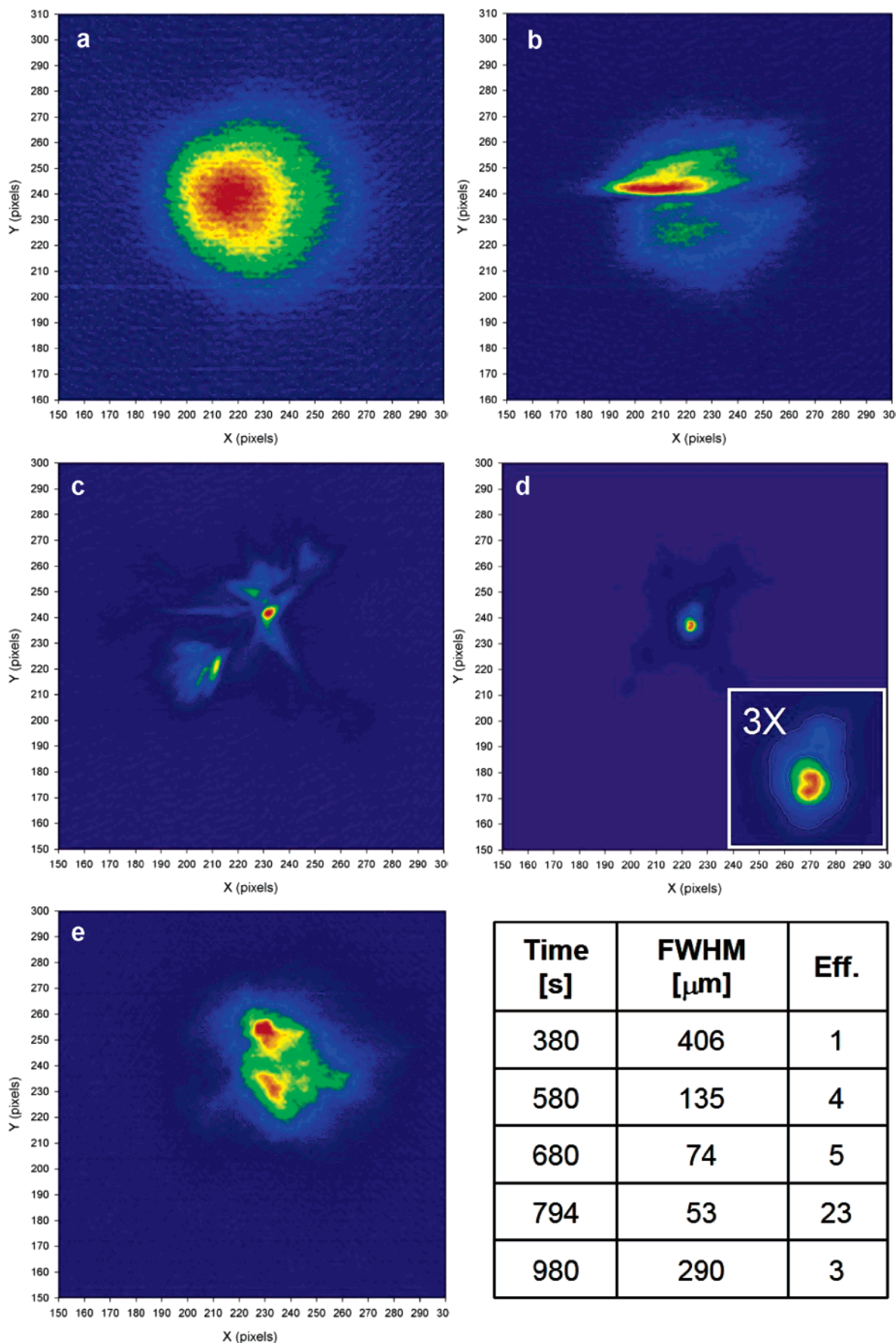


Figure 6. Changes in the spatial profile of a white light beam at $22.0 \text{ W}\cdot\text{cm}^{-2}$ propagating in an organosiloxane sol that was simultaneously irradiated with a uniform optical field at (a) 380 s, (b) 580 s, (c) 680 s, (d) 794 s, and (e) 980 s. A table summarizing the beam widths (fwhm, y direction) and self-trapping efficiency corresponding to the images is included.

example, trapping of the beam under the external field was not observed for times < 500 s; in separate experiments in gels that were pre-irradiated for times < 500 s, the white light beam also remained diffracted and did not self-trap. Even more strikingly, the largest value of the maximum efficiency of self-trapping was obtained in gels irradiated for 800 s; under the external optical field, the maximum efficiency is reached after irradiation for 794 s.

Summary and Outlook

Self-trapped beams of white light with similar spatial profiles at intensities ranging across an order of magnitude were generated due to photoinitiated free-radical polymerization in an organosiloxane medium. The dynamics of the self-trapped beams including the rate of self-trapping in stage (i), the average duration of oscillations in stage (ii), and the efficiency of self-induced waveguides in stage (iii) were found to be strongly correlated to the kinetics of free-radical polymerization—in other words, the rates of refractive index changes—in the organosiloxane medium. Furthermore, the dynamics of self-trapped white light beams is strikingly similar to self-trapped solutions derived for coherent monochromatic light. These studies provide accessible photochemical routes to self-trapped beams of white light, which are extremely difficult to generate in media with nonlinearities based on higher-order susceptibility tensors. By controlling the polymerization kinetics in the medium (by varying optical intensity *or* the concentration of polymerizable groups), it should be possible to tune the dynamics of the self-trapped beams. These findings could enable the empirical testing

of the intriguing predictions made by new theoretical models of the behavior of self-trapped incoherent beams including unusual forms of interactions of self-trapped beams and the spontaneous disintegration of collimated white light into periodic patterns.⁷ Although modulation instability-seeded white light patterns were recently observed in a photorefractive crystal,⁴⁶ many of these phenomena, which occur in the same parameter range as self-trapped beams, remain to be discovered in the realm of spatially and temporally incoherent light.

Acknowledgment. We gratefully acknowledge funding from NSERC, CFI/OIT and McMaster University. We thank CIBA-GEIGY, Canada for donation of the photoinitiator IRGACURE 784. K.S. thanks Mr. John Lannan for calculations of Gaussian beam profiles and Prof. J. Preston and Dr. A. Knights (Department of Engineering Physics, McMaster) for valuable discussions.

Supporting Information Available: Experimental details, comparison of Gaussian profile with $\text{fwhm} = 45 \mu\text{m}$ before and after averaging by 150 nm steps, two-dimensional intensity profiles of self-trapped beams at 7.9 and $5.4 \text{ W}\cdot\text{cm}^{-2}$, plots and table of parameters corresponding to the temporal evolution of self-trapping in organosiloxane gels with different extents of polymerization, temporal plot of self-trapping efficiency and beam width under a uniform external field. This material is available free of charge via the Internet at <http://pubs.acs.org>.

JA0645335

(46) Schwartz, T.; Carmon, T.; Buljan, H.; Segev, M. *Phys. Rev. Lett.* **2004**, *93*, 223901-1–223901-4.